

Study of Dark-Conductivity and Photoconductivity of ZnO Nano Structures Synthesized by Thermal Decomposition of Zinc Oxalate

Ravi Shankar, Rajneesh K. Srivastava,* and S. G. Prakash

Department of Electronics and Communication, University of Allahabad, Allahabad-211002, India

(received date: 22 September 2012 / accepted date: 29 January 2013 / published date: 10 September 2013)

In the present work, zinc oxalate $[ZnC_2O_4 \cdot 2H_2O]$ was used as precursor to prepare zinc oxide nano structures by thermal decomposition. Its photoconductivity and dark-conductivity properties have been studied in air as well as in vacuum. Voltage dependence of photocurrent and dark-current has been observed at room temperature in air under UV-vis illumination and is found as superlinear in nature. Rise and decay curve in air exhibits anomalous behavior wherein the photocurrent decreases even during steady illumination. In vacuum, the rise of photocurrent becomes slow and prolonged.

Keywords: photoconductivity, zinc oxalate, zinc oxide, thermal decomposition

1. INTRODUCTION

Photoconductivity is defined as electrical conductivity resulting from photo-induced electron excitations in which light is absorbed. In semiconductors, photoconductivity arises due to photo-generation of electron hole pairs after absorption of photons which increases carrier density and conductivity of material.^[1-4] Photoconductivity is an important tool to study the properties of semiconducting materials such as the nature of photo-excitation and recombination processes. Photoconductivity of material depends on the carrier density, carrier lifetime and complex process of carrier generation, trapping and recombination. Photoconductivity is also a function of temperature, applied field, intensity of light and energy of radiation.^[5-6] Extensive study of photoconductivity has been made in nanoparticles, thin film, nanorods, nanowires and mixed lattice^[7-13] for different parameters. However, only few attempts have been made using thick film of powdered layer without any binder which is simple and economical.

Zinc oxide (ZnO) is a material of particular interest because it possesses unique optical and electrical properties. It is a wide-band semiconductor (3.37 eV) and is a good candidate for many applications.^[14-17] For example thin films of ZnO were reported to display good photoconductivity and high transparency in visible region and has been used as transparent electrodes for solar cells.^[18] It is also used prominently for its application as an ultraviolet (UV) light detector.^[19] Many authors have reported photoconductivity in ZnO thin films, nanorods, nanowires, nanoparticles and

thick films.^[20-23] A number of synthesis methods have been used to synthesize ZnO nano structures such as chemical vapour deposition, sol-gel, spray pyrolysis, co-precipitation, thermal decomposition and hydrothermal methods.^[24,25] Thermal decomposition is a simple, low-cost and mass-scale production method. There are a number of reports on synthesis of ZnO nano structures by thermal decomposition of zinc nitrate, zinc acetate, zinc sulfate, zinc hydroxide etc.^[26,29] ZnO nano structures synthesized by thermal decomposition of zinc oxalate have been studied by several authors^[27-31] for their emission and optical properties.

In the present work ZnO nano structures synthesized by thermal decomposition of Zinc Oxalate have been studied for their photoconductivity properties by observing variation of photocurrent and dark-current as a function of applied voltage and time in air as well as in vacuum under ultraviolet-visible (UV-vis) illumination. Structural and morphological studies also have been performed for synthesized ZnO nano structures. Study of photoconductivity in ZnO nanostructures synthesized by thermal decomposition of zinc oxalate is, perhaps, first of its kind to the best of our knowledge.

2. EXPERIMENTAL PROCEDURE

Zinc oxalate ($ZnC_2O_4 \cdot 2H_2O$) (purity: 99%) was procured from E. Merck Ltd., Mumbai, and was directly used without special treatment.

The Zinc Oxalate was used as precursor to synthesize ZnO nano structures. About 2 g of zinc oxalate was placed in a crucible and was calcined at 500°C in a muffle furnace for 3 h. ZnO nano structures were obtained in powder form.

The crystal structure of ZnO nano structures was characterized by x-ray diffraction (XRD) using PANalytical

*Corresponding author: rkumarsau@gmail.com
©KIM and Springer

system, and scanning electron microscope (SEM) images were obtained using JEOL scanning electron microscope. For photoconductivity and dark-conductivity measurements, a cell was formed by spreading a thick layer of powdered sample between Cu electrodes etched on a Cu plate printed circuit board. The powdered layer was pressed with transparent glass plate. In the cell, the direction of illumination is normal to field across the electrodes. The cell was mounted in a dark chamber with a slit where the light was allowed to fall over the cell. UV-vis photo-response was measured using a Hg lamp of 300 W as a photo-excitation source and current was measured using RISH Multi 15S with adapter RISH Multi SI 232. The light intensity over the cell surface was changed by varying the distance between slit and light source. Before measuring photoconductivity of the sample, the cell was first kept in dark till it attained equilibrium. For measuring photoconductivity in vacuum, we used Tarson Rockyvac 300 vacuum pump to create vacuum in a glass chamber.

3. RESULTS AND DISCUSSION

Figure 1 shows the XRD pattern of ZnO nano structures prepared by thermal decomposition of zinc oxalate at 500°C for 3 h. All the diffraction peaks can be indexed to the ZnO wurzite structure corresponding to JCPDS card No. 75-0576. No other characteristic peaks of impurities, such as Zn(OH)₂, were observed indicating that the prepared ZnO is of high purity. Similar results have been reported by C.W. Yao *et al.*^[31] Crystallite size (D) of the sample was calculated using Debye Scherrer formula:^[32]

$$D = \frac{0.9\lambda}{\beta \cos \theta} \quad (1)$$

where β is full width at half maximum (FWHM) in radians, λ is the x-ray wavelength (1.542 Å of Cu $K\alpha$) and θ is the

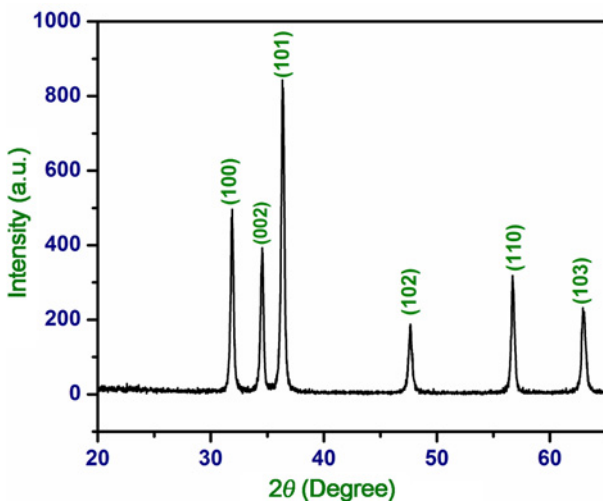


Fig. 1. XRD pattern of synthesized ZnO nano structures.

Bragg's angle. The crystallite size calculated for first three peaks is 32 nm, 32 nm, and 31 nm respectively.

Figures 2(a) and 2(b) show the SEM images of synthesized ZnO nano structures. The nano structures of zinc oxide consists of irregular cuboids formed by a large number of rectangular platelets with an average length and width of around 1000 nm and 30 nm, respectively. Similar morphology has been reported for zinc oxalate dihydrate prepared from zinc sulfate by Justin *et al.*^[33]

Figure 3 shows UV-visible absorption spectra of bulk ZnO as well as nanostructure of ZnO. The absorbance peak is at 383 nm and 386 nm for nanostructure of ZnO and bulk ZnO respectively. This blue shift of absorbance peak may be attributed to nano dimensions of ZnO.^[34]

Figure 4 shows FTIR spectrum of ZnO nanostructures. The band located near 567 cm⁻¹ can be attributed to the ZnO stretching mode.^[35] A broadband near 3130 cm⁻¹ exhibits presence of -OH groups on the surface of nanostructures of ZnO.^[36] The peaks observed at 1631 cm⁻¹ and 1404 cm⁻¹ are

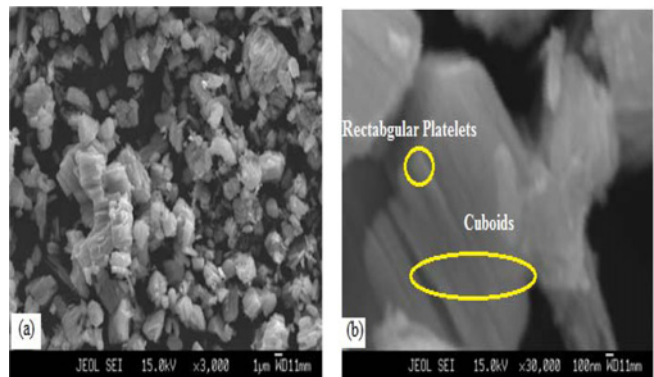


Fig. 2. SEM image of ZnO nano structures (a) at low magnification and (b) at high magnification.

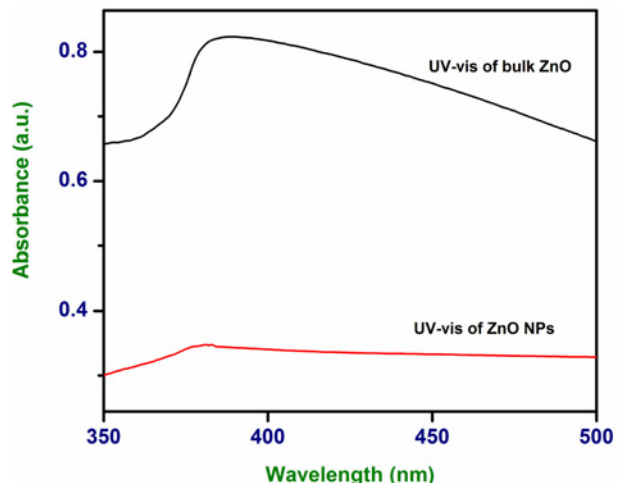


Fig. 3. UV-visible absorption spectra of synthesized ZnO nano structures and bulk ZnO.

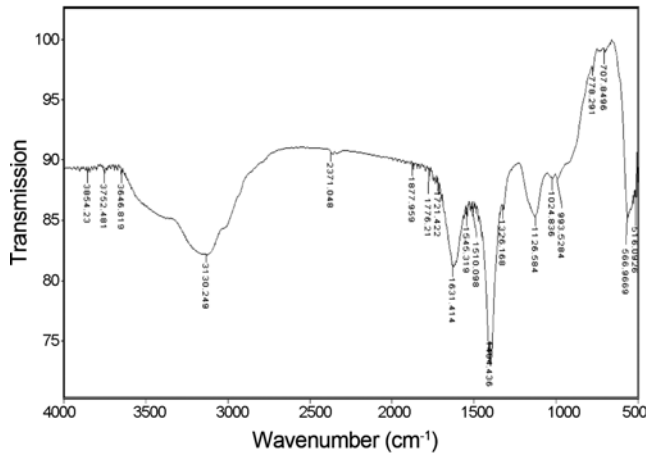


Fig. 4. FTIR spectrum of synthesized ZnO nano structures.

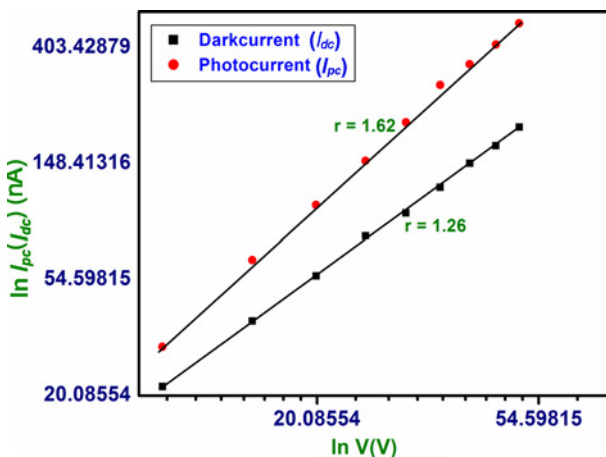


Fig. 5. Variation of photocurrent and darkcurrent as a function of applied voltage for ZnO nano structures.

due to the asymmetrical and symmetrical stretching of zinc carboxylate.^[37]

Figure 5 shows the variation of dark-current (I_{dc}) and photocurrent (I_{pc}) with voltage of ZnO nano structures on ln–ln scale. Under UV-vis illumination, $\ln(I)$ versus $\ln(V)$ curves are straight lines. Thus the variation of dark-current and photocurrent as a function of voltage can be represented by power law $I \propto V^r$, where I is photocurrent (I_{pc}) or darkcurrent (I_{dc}), V is DC biasing voltage and r is slope of a straight line section.^[3-5] The dependence of dark-current (I_{dc}) as well as that of photocurrent (I_{pc}) with applied voltage is found to be superlinear ($r > 1$). The superlinear variation suggests that some additional charge carriers were being injected into the materials from one of the electrodes.^[38]

Figure 6 shows rise and decay curve of photocurrent under UV illumination in air with fixed photo flux and bias voltage. The cell was initially kept in dark till the dark-current was stabilized. When the light was switched on, the

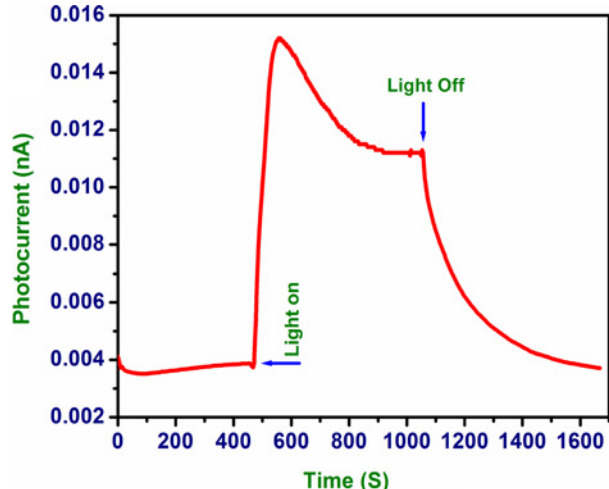


Fig. 6. Rise and decay of ZnO nano structures in air.

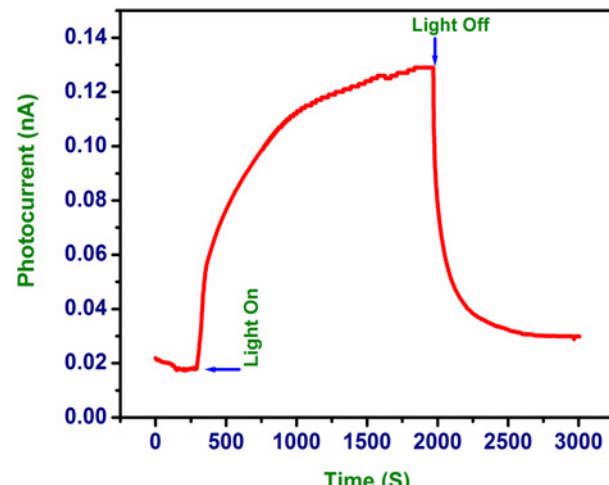
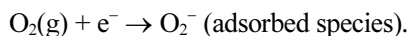


Fig. 7. Rise and decay of ZnO nano structures in vacuum.

photocurrent initially increased very fast due to the quick generation of electron and hole pairs as a result of absorption of photons. After attaining a peak, the photocurrent started to decrease slowly even during illumination. This kind of anomalous behavior may be attributed to slow process of photoinduced chemisorption of oxygen molecules on the surface of ZnO nano structures.^[39] Oxygen molecules get adsorbed on the surface as follows:



When the light was switched off the current decreased very fast initially, which could be attributed to recombination of free electrons and holes.^[1] Later, the current decreased slowly, which could be attributed to slow process of desorption of oxygen molecules as follows:



Figure 7 shows the variation of photocurrent in vacuum.

When UV light was switched on, the photocurrent initially increased very fast. Later the rate of increase of photocurrent reduced. Eventually the photocurrent reached to a steady state but in more than 30 min. This comparatively slow and prolonged response in vacuum may not be attributed to the desorption of oxygen molecules on the surface of ZnO nano structures. Instead carbon-catalyzed photolysis of ZnO nano structures resulting in slow increase of lattice oxygen as suggested by Bao *et al.*^[39] may be responsible for such slow and prolonged rise as evidenced by the participation of carbon in thermal decomposition of zinc oxalate as follows:



The process is found to be reversible by exposure to gaseous oxygen in the dark. The steady state value of photocurrent in vacuum is higher than the photocurrent in air by an order of 1. This may be attributed to increased dark current in vacuum which is also higher than the dark current in air by an order of 1. The high dark-current in vacuum may be attributed to the increased concentration of free electrons as a result of non-availability of oxygen molecules in vacuum to be adsorbed on the surface of ZnO nano structures by capturing free electrons. Bao *et al.*,^[39] Ahn *et al.*^[40] and Li *et al.*^[41] have also reported increase in darkcurrent in vacuum in ZnO nanowires. When the light is switched off, the decay of current in vacuum is fast as compared to that in air. This may be due to absence of slow process of desorption of oxygen molecules. The slow portion of decay may be due to the presence of traps.^[12]

The trap depth is calculated by peeling off the decay portion of the rise and decay curve. Decay is expressed as follows:^[3,42,43]

$$I = I_0 \exp(-pt) \quad (4)$$

where, p is the probability of escape of an electron from the trap per second, I_0 is the current at the time when light is switched off and I is photocurrent at time ' t ' after the light is switched off. The probability of an electron escaping from a trap is also given by relation:

$$p = S \exp(-E/kT) \quad (5)$$

where, k is Boltzman constant (1.381×10^{-23} J/K), T is absolute temperature and S is the frequency factor i.e. attempt to escape frequency.^[22] The attempt to escape frequency (S) may be defined as the number per second that the quanta from crystal vibrations (phonons) attempt to eject electrons from the traps, multiplied by the probability of transition from trap to conduction band. 'S' is of the order of 10^9 at room temperature as reported by Randall and Wilkins.^[44] From Eqs. (4) and (5), trap depth (E) can be expressed as follows:

$$E = kT \left[\log_e S - \log_e \frac{\log_e(I_0/I)}{t} \right].$$

The trap depth is calculated from decay portion of curve shown in Fig. 7 and is 0.65 eV.

4. CONCLUSIONS

In the present work, ZnO nano structures were synthesized by thermal decomposition of zinc oxalate ($\text{ZnC}_2\text{O}_4 \cdot 2\text{H}_2\text{O}$) at 500°C for 3 h. This method is inexpensive and reproducible for synthesis of ZnO nano structures in mass scale. X-ray diffraction (XRD) result shows that the prepared samples have hexagonal wurzite structure of ZnO and the estimated size is around 32 nm. SEM images show formation of rectangular platelets arranged in a form of irregular cuboids. Photocurrent and darkcurrent were found to vary superlinearly with applied voltage. The photocurrent in vacuum is higher than that in air by an order of 1. Photocurrent in vacuum does not decrease after attaining its peak during steady illumination whereas photocurrent in air decreases after attaining its peak. Photocurrent in vacuum was found to rise slowly for prolonged duration.

ACKNOWLEDGEMENTS

One of the authors, Rajneesh K. Srivastava, is thankful to UGC for its support in the form of a project grant (No. 37-395/2009 (SR)). The authors are thankful to National Centre of Experimental Mineralogy and Petrology, University of Allahabad, Allahabad for providing XRD and SEM measurements.

REFERENCES

- R. H. Bube, *Photoconductivity of Solids*, p. 404, John Wiley, New York (1967).
- R. H. Bube, *Photoelectronic Properties of Semiconductors*, p. 18, Cambridge University Press, New York (1992).
- S. K. Mishra, R. K. Srivastava, S. G. Prakash, R. S. Yadav, and A. C. Panday, *Opto-Electron. Rev.* **18**, 467 (2010).
- R. K. Srivastava and S. G. Prakash, *Natl. Acad. Sci. Lett.* **30**, 11 (2007).
- S. Srivastava, S. K. Mishra, R. S. Yadav, R. K. Srivastava, A. C. Panday, and S. G. Prakash, *Dig. J. Nanomater. Bios.* **5**, 161 (2010).
- J. A. Schmidta, C. Longeaud, R. R. Koropecki, and J. P. Kleider, *J. Non-Cryst. Solids* **352**, 1024 (2006).
- S. Mridha and D. Basak, *Chem. Phys. Lett.* **427**, 62 (2006).
- P. Sharma, K. Sreenivas, and K. V. Rao, *J. Appl. Phys.* **93**, 3963 (2003).
- S. Sapra and D. D. Sarma, *Phys. Rev. B* **69**, 125304 (2004).
- J. Wang and L. Gao, *J. Cryst. Growth* **262**, 290 (2004).

11. O. Harnack, C. Pacholski, H. Weller, A. Yasuda, and J. M. Wessels, *Nano Lett.* **3**, 1097 (2003).
12. R. Kripal, A. K. Gupta, R. K. Srivastava, and S. K. Mishra, *Spectrochim. Acta A* **79**, 1605 (2011).
13. L. Nurtdinova, V. Semashko, Y. Guyot, S. Korableva, M. F. Joubert, and A. Nizamutdinov, *Opt. Mater.* **33**, 1530 (2011).
14. S. K. Mishra, S. Srivastava, R. K. Srivastava, A. C. Panday, and S. G. Prakash, *Adv. Mater. Lett.* **2**, 298 (2011).
15. S. K. Mishra, R. K. Srivastava, and S. G. Prakash, *J. Mater. Sci.-Mater. El.* **24**, 125 (2013).
16. Z. L. Wang, *Mater. Sci. Eng.* **64**, 33 (2009).
17. S. K. Mishra, R. K. Srivastava, S. G. Prakash, R. S. Yadav, and A. C. Panday, *J. Alloy. Compd.* **513**, 118 (2012).
18. T. Markvart and L. Castaner, *Solar Cells: Materials, Manufacture and Operation*, p. 32, Elsevier, Great Britain (2006).
19. P. Sharma, A. Mansingh, and K. Sreenivas, *Appl. Phys. Lett.* **80**, 553 (2002).
20. Y. Natsume, H. Sakata, T. Hirayama, and H. Yanagida, *J. Appl. Phys.* **72**, 4203 (1992).
21. T. Okamura, Y. Seki, S. Nagakary, and H. Okushi, *Jpn. J. Appl. Phys.* **31**, L762 (1992).
22. R. Kripal, A. K. Gupta, S. K. Mishra, R. K. Srivastava, A. C. Pandey, and S. G. Prakash, *Spectrochim. Acta A* **76**, 523 (2010).
23. T. Ahmad, S. Vaidya, N. Sarkar, S. Ghosh, and A. K. Ganguli, *Nanotechnology* **17**, 1236 (2006).
24. J. Aranovich, A. Ortiz, and R. H. Bube, *J. Vac. Sci. Technol.* **16**, 994 (1979).
25. R. S. Yadav and A. C. Pandey, *J. Exp. Nanosci.* **2**, 177 (2007).
26. M. Bitenc, M. Marinšek, and Z. C. Orel, *J. Eur. Ceram. Soc.* **28**, 2915 (2008).
27. L. Shen, N. Bao, K. Yanagisawa, K. Domen, A. Gupta, and C. A. Grimes, *Nanotechnology* **17**, 5117 (2006).
28. C. K. Srikanth and P. Jeevanandam, *J. Alloy Compd.* **486**, 677 (2009).
29. N. Audebrand, J. Auffredic, and D. Louer, *Chem. Mater.* **10**, 2450 (1998).
30. R. Vaidhyanathan, S. Natrajan, and C. N. R. Rao, *J. Chem. Soc.*, 699 (2001).
31. C. W. Yao, H. P. Wu, M. Y. Ge, L. Yang, Y. W. Zeng, Y. W. Wang, and J. Z. Jiang, *Mater. Lett.* **61**, 3416 (2007).
32. B. D. Culty, *Elements of X-ray Diffraction*, p. 149, Addison-Wesley, New York (1978).
33. C. J. Raj, R. K. Joshi, and K. B. R. Varma, *Cryst. Res. Technol.* **46**, 1181 (2011).
34. K. Rekha, M. Nirmala, M. G. Nair, and A. Anukalian, *Physica B* **405**, 3180 (2010).
35. R. Viswanatha, T. G. Venkatesh, C. C. Vidyasagar, and Y. A. Nayaka, *Arch. Appl. Sci. Res.* **4**, 480 (2012).
36. A. Abdolmaleki, S. Mallakpour, and S. Borandeh, *Appl. Surf. Sci.* **257**, 6725 (2011).
37. G. Xiong, U. Pal, J. G. Serrano, K. B. Ucer, and R. T. Williams, *Phys. Status Solidi C* **3**, 3577 (2006).
38. R. W. Smith and A. Rose, *Phys. Rev.* **97**, 1531 (1955).
39. J. Bao, I. Shalish, Z. Su, R. Gurwitz, F. Capasso, X. Wang, and Z. Ren, *Nanoscale Res. Lett.* **6**, 404 (2011).
40. S. E. Ahn, H. J. Ji, K. Kim, G. T. Kim, C. H. Bae, S. M. Park, Y. K. Kim, and J. S. Ha, *Appl. Phys. Lett.* **90**, 153106 (2007).
41. Q. H. Li, T. Gao, Y. G. Wang, and T. H. Wang, *Appl. Phys. Lett.* **86**, 123117 (2005).
42. S. Devi and S. G. Prakash, *J. Phys.* **39**, 145 (1992).
43. R. Ghosh and D. Basak, *J. Appl. Phys.* **101**, 113111 (2007).
44. J. F. Randal and J. H. F. Wilkins, *Proc. Royal Soc. A* **184**, 366 (1945).